

Auto-Calibrating Adaptive Array for Mobile Telecommunications

Mattias Wennström, Jonas Strandell, Tommy Öberg, Erik Lindskog and Anders Rydberg

15th August 2000

Abstract

A major concern for adaptive antennas is the calibration of hardware. Here we consider the calibration of an analog beamformer, which calculates the weights in a DSP, but weights the RF signals using a hardware beamformer. This paper presents two novel methods of performing a calibration of this adaptive antenna during normal operation. This will mitigate temperature drift and aging of active components. Both methods use a feedback of the beamformer output signal, to calculate the error in the beamformer output, or to identify the parameters in the temperature drift. The algorithms are transparent to normal antenna operation and are computationally simple. Simulations show that when using these auto-calibration methods, the performance is independent of variation in hardware parameters when a realistic temperature drift is introduced. The proposed algorithms are intended for use in a TDMA mobile telephone system, but the methods are applicable in radar systems also.

1 Introduction

The benefits of using an adaptive array antenna at the basestation site in a mobile telecommunication system in order to increase spectral efficiency is well known [1],[2]. In this paper an important issue in array technology is addressed, namely the calibration of the antenna array. Calibration of antenna arrays for mobile communication systems has earlier been presented in [3]. There the sensitivity of a digital beamforming system to calibration errors were studied and a method to calibrate the array prior to operation was presented. In [4] an auto-calibration algorithm for the transmitter part of a digital beamformer was presented.

In this paper, the uplink, or receiving part of the array antenna in a TDMA system, as for example GSM, is considered. It is also assumed that we use an analog beamformer (ABF), where the beamformer weights are calculated in a digital signal processor (DSP), but the weighting is performed by hardware weighting units on the RF signals. The benefits of using an ABF as compared to the digital beamformer, where both weight calculation and beamforming is

performed in the DSP, is that the beamformer output signal can be connected to an ordinary basestation receiver. The proposed system can thus be used as an add-on system to existing basestations to improve system performance in "hot-spot" traffic areas.

When using the ABF, it is important to know the transfer function between the input sampling receivers and the point in the signal path where the weights are applied to the signals, to be able to compensate for this difference. Prior to start-up, this transfer function is measured using an off-line calibration algorithm. However, there are active components in the weighting units and the receivers, which are sensitive to temperature variations and whose characteristics also will change due to aging. This will soon make the off-line calibration data invalid.

In Figure 1, measurements of the temperature drift in amplitude and phase for the hardware weighting unit used in an ABF testbed described in [5],[6], is presented. The measurements were performed over a period of ten hours after a cold start-up. We can see that the drift is approximately 0.1 dB and 1° per hour of operation and it demonstrates the need for frequent re-calibrations. It is therefore desirable if the calibration can be performed simultaneous with normal antenna operation.

This paper presents two on-line calibration algorithms, that are transparent to normal antenna operation and have low complexity. The first algorithm is derived from the least mean square (LMS) algorithm and is a non-parametric solution. The second algorithm is derived using a parametric approach, where the transfer function is identified and the temperature drift is tracked. To study the performance of the proposed algorithms, a simulation was performed, modeling a simple signal environment with two signal sources (mobiles) and no multipath propagation. The time variations in the hardware was simulated by using a parameter drift similar to the measured one. Both algorithms succeed to maintain the output signal to interference ratio (SIR) at the same level as with perfect knowledge of the transfer functions. The LMS-like algorithm requires a slowly or non-varying signal environment, while the second algorithm actually benefits from a rapidly varying signal environment, which is characteristic for fading in a multipath scenario.

The paper is organized as follows, in Section 2, the

model of the hardware in the adaptive antenna is introduced and the sample matrix inversion (SMI) algorithm is described. In Section 3, the proposed auto-calibration algorithms are described and in Section 4 the simulation results are presented. Finally the results are summarized in Section 5.

2 Problem formulation

A block diagram of the adaptive antenna is shown in Figure 2. The signals arriving at the N antennas are described by the $N \times 1$ column vector $\mathbf{x}_a(t)$. The noise generation in the front end is modeled as a zero mean white Gaussian noise vector, $\mathbf{n}_1(t)$, with covariance matrix $\sigma_1^2 \mathbf{I}$. The noise in the input down-converting and sampling receivers, $\mathbf{n}_2(t)$ is also modeled as a zero mean white Gaussian noise vector, but with covariance matrix $\sigma_2^2 \mathbf{I}$. The signals from the antennas are split into a digital path and an analog path. The analog path consists of cables and the hardware weighting units. The digital part consists of digital signal processing for weight computation and calibration.

Assuming all weights are set to unity, the transfer function measured between the input sampling receiver at point A in Figure 2 and the beamformer weighting units, point B , is described by the complex diagonal matrix $\mathbf{D} = \text{diag}[d_1, \dots, d_N]$. The signals at the beamformer is denoted $\mathbf{x}''(t)$ and is defined as $\mathbf{x}''(t) = \mathbf{D}\mathbf{x}(t)$. Each factor d_l describes the attenuation and the phase shift of the analog path l relative to the corresponding digital path, except for the noise $\mathbf{n}_2(t)$.

The factors d_l will in general be nonlinear functions of the calculated weights, \mathbf{w} , due to coupling between the phase shifters and the attenuators. The matrix \mathbf{D} will thus in general be a nonlinear function of \mathbf{w} , i.e. $\mathbf{D} = \mathbf{D}(\mathbf{w})$. The elements in \mathbf{D} are assumed to be constant over the receiver passband, but they will change during operation due to temperature drift in the weighting units, as seen experimentally in Figure 1.

The output from the beamformer is down-converted to the baseband and sampled giving $\hat{y}(k) = y(t_k) + n_3(t_k)$. The notation t_k will be used in this paper, to denote the time continuous signal sampled at the time instant $t = t_k$. The term $n_3(t)$ is the noise added by the feedback receiver. We will assume that $n_3(t)$ is zero mean complex Gaussian with variance σ_3^2 . The signal $\hat{y}(k)$ will be used in the calibration algorithms, to be presented below.

2.1 The SMI-algorithm

The example antenna presented here uses the Sample Matrix Inversion (SMI)-algorithm to calculate the

adaptive antenna weights. A reference signal, $s(k)$, present in each transmitted burst, e.g. the training sequence in a Time Division Multiple Access (TDMA)-systems like GSM and IS-136, is utilized in order to form a least-squares problem. The sampled baseband signals of the antenna elements form a column vector denoted $\mathbf{x}'(k)$. The mean square optimal weight vector is obtained by solving the Wiener-Hopf equations [7].

$$\hat{\mathbf{w}}_0 = \hat{\mathbf{R}}_{\mathbf{x}\mathbf{x}}^{-1} \hat{\mathbf{r}}_{\mathbf{x}s} \quad (1)$$

where the sample-mean covariance matrix and cross-correlation vector are estimated by using M samples as

$$\begin{aligned} \hat{\mathbf{R}}_{\mathbf{x}\mathbf{x}} &= \frac{1}{M} \sum_{k=1}^M \mathbf{x}'(k) \mathbf{x}'^H(k) \\ \hat{\mathbf{r}}_{\mathbf{x}s} &= \frac{1}{M} \sum_{k=1}^M \mathbf{x}'(k) s^*(k) \end{aligned} \quad (2)$$

Here, $(\cdot)^H$ denotes complex conjugate transpose and $(\cdot)^*$ denotes complex conjugate. The SMI-algorithm tries to combine the N antenna signals in an optimum way, given the structure. There is no need to estimate the direction of arrival for the impinging signals, so a calibration of the array manifold (the common path) is not necessary.

2.2 Calibration

Compensation of phase and magnitude differences between the digital path and analog path must be performed for each antenna element, since the adaptive antenna weights are calculated based on the sampled signals of the digital paths, $\mathbf{x}'(k)$, whereas the beamforming is performed on the RF-signals of the analog paths $\mathbf{x}''(t)$.

Prior to operation, the matrix \mathbf{D} is computed by performing a calibration. This calibration step is called an off-line calibration and the corresponding matrix is denoted \mathbf{D}_0 . A continuous wave (CW) signal at the carrier frequency is injected at one antenna element at a time by directional couplers. The attenuation and the relative phase of that specific analog path compared to the digital path can be measured by using the signal $\hat{y}(k)$. The calibration process is then repeated for all N antenna branches.

If the magnitude of a weight is adjusted, the adjusted phase will also change, and vice versa, due to non-ideal isolation between the phase shifter and the attenuator in the hardware weights. The relation between the desired and the actual weight used for weight control is stored in a look-up table with all possible weight settings as entries. Since full access to the control of the weighting units is required, the off-line calibration can only be performed prior to operation of the adaptive antenna.

During operation, temperature drift in the receivers and weighting units and other possible changes will degrade the performance of the adaptive antenna. It is therefore desirable to perform some calibration simultaneously with the main operation. This calibration must be of relatively low complexity and yet accurate enough to maintain a good performance of the adaptive antenna. Furthermore, the calibration should not interfere with the main operation of the antenna.

3 The auto-calibrating algorithms

3.1 The LMS-approach

This section outlines the auto-calibration algorithm using an LMS-approach and presents the assumptions made concerning the off-line calibration and the thermal drift of the involved hardware.

A signal-flow graph of the proposed algorithm is shown in Figure 3. The signals at the weighting units, $\mathbf{x}''(t)$, are multiplied with the weight-vector $\hat{\mathbf{w}}^H(p-1)$, based on the calculations in the previous frame $p-1$, where p is the frame index, i.e. $y(t) = \hat{\mathbf{w}}^H(p-1)\mathbf{x}''(t)$. Since adaptive arrays utilizing analog beamforming is studied, the weights are assumed to be applied to the data of the next TDMA frame. This is necessary since otherwise the weights have to be calculated and steered out during a time period that is much shorter than a frame. This also implies that the time step in the algorithm is one TDMA frame.

The sampled beamformer output signal, $\hat{y}(k)$, is compared with the corresponding beamformer output signal in the DSP, $y_0(k)$, and the error signal $e(k) = y_0(k) - \hat{y}(k)$ is formed. The signal $y_0(k)$ is calculated by using the SMI-weights from the previous frame as $y_0(k) = \hat{\mathbf{w}}_0^H(p-1)\mathbf{x}'(k)$. However, only one sample k is used and it can be taken arbitrarily from the whole frame p .

For calculation of the necessary adjustments an LMS-like (least mean square) algorithm is proposed. The aim of the algorithm is to minimize the mean squared magnitude of the error signal $e(k)$.

We assume that the signal vector $\mathbf{x}''(t_k)$ relates to $\mathbf{x}'(k)$ according to

$$\mathbf{x}''(t_k) = \mathbf{D}\mathbf{x}(t_k) = \mathbf{D}\{\mathbf{x}'(k) - \mathbf{n}_2(k)\} \quad (3)$$

The relationship between $\mathbf{D}\mathbf{x}(t_k)$ and $\mathbf{x}'(k)$ in (3) is an approximation, since $\mathbf{D} = \mathbf{D}(\mathbf{w})$ and \mathbf{w} in turn depends on $\mathbf{x}'(k)$. We thus assume here that the matrix \mathbf{D} is independent of the weights. It is possible to accomplish this by designing the hardware weights with high isolation between the phase shifter and the attenuator.

To adjust the weights to compensate for the temperature drift, the well known LMS-approach would use

$\mathbf{x}''(t_k)$ and $e(k)$ to update the weight vector as:

Desired algorithm: ($p \geq 1$)

$$\begin{aligned} y_0(k) &= \hat{\mathbf{w}}_0^H(p-1)\mathbf{x}'(k) \\ e(k) &= y_0(k) - y(t_k) \\ \hat{\mathbf{w}}(p) &= \hat{\mathbf{w}}(p-1) + \mu\mathbf{x}''(t_k)e^*(k) \end{aligned} \quad (4)$$

Where the initialization of the algorithm has been omitted.

The constant μ is the step-size parameter in the algorithm and $y(t)$ is the output of the analog beamformer. The algorithm (4) cannot be used since $\mathbf{x}''(t_k)$ is not measurable and only a noisy estimate of $y(t_k)$ is available. The approach used here is therefore to use $\mathbf{x}'(k)$, i.e. the noisy measurement of $\mathbf{x}(k)$, and the matrix \mathbf{D}_0 obtained from the off-line calibration process to estimate $\mathbf{x}''(t_k)$, using (3). The proposed algorithm can then be stated as follows:

Proposed algorithm:

Initialization: ($p=0$)

$$\hat{\mathbf{w}}(0) = (\mathbf{D}_0^{-1})^H \hat{\mathbf{w}}_0(0) \quad (5)$$

Algorithm: ($p \geq 1$)

$$\begin{aligned} y_0(k) &= \hat{\mathbf{w}}_0^H(p-1)\mathbf{x}'(k) \\ \hat{e}(k) &= y_0(k) - \hat{y}(k) \\ \mathbf{x}''(k) &= \mathbf{D}_0\mathbf{x}'(k) \\ \hat{\mathbf{w}}(p) &= \hat{\mathbf{w}}(p-1) + \mu\mathbf{x}''(k)\hat{e}^*(k) \end{aligned} \quad (6)$$

The fact that the calibration data from the off-line calibration is used will only slightly affect the performance of the gradient method since the LMS-approximation of the gradient is in itself very crude. The correct instantaneous gradient direction is given by $\mathbf{x}''(t_k)e^*(k)$ but here the approximation $\mathbf{D}_0\mathbf{x}'(k)\hat{e}^*(k)$ is used instead. An exact analysis of the influence of the properties of this error in gradient estimate on the convergence of the algorithm remains to be investigated. Simulation studies presented in Section 4 show that the performance of the proposed algorithm will be satisfactory in a relatively stationary signal environment, i.e. with a slowly varying SMI-weight vector. When the signal environment is non stationary, the long convergence time inherent in LMS-like algorithms can be expected to create problems. The error term $\hat{e}(k)$ will be large if the SMI-weight vector \mathbf{w}_0 is not changing slowly. The performance will then be degraded.

3.2 The tracking approach

An alternative on-line calibration method is to track the temperature drift of the transfer functions d_l , $l = 1, \dots, N$, to form the estimated row-vector $\hat{\mathbf{d}}(p) = [\hat{d}_1(p)\hat{d}_2(p)\dots\hat{d}_n(p)]$. The idea is to consider the output signal $y(t_k)$ as a linear combination of the signals $\mathbf{z}(t_k)$, after the weights, $\hat{\mathbf{w}}$, as in Figure 4. Note

that the order of the weights and the transfer function coefficients d_l has been switched. However, only $\mathbf{x}'(k)$ and $\hat{y}(k)$ can be measured, and not $\mathbf{z}(t_k)$ and $y(t_k)$. By using the known weights and the identified transfer function vector from the previous frame, $\hat{\mathbf{d}}(p-1)$, we can estimate $\mathbf{z}(t_k)$. The estimate is denoted by $\mathbf{z}(k)$ and element l in the column vector $\mathbf{z}(k)$ is defined as:

$$\begin{aligned} z_l(k) &= x'_l(k) \hat{w}_l^*(p-1) \\ &= x'_l(k) \frac{\hat{w}_{0,l}^*(p-1)}{\hat{d}_l(p-1)} \end{aligned} \quad (7)$$

This regressor vector is now used in the identification of \mathbf{d} by forming a least-squares identification problem utilizing the sampled output $\hat{y}(k)$. This approach is possible since the system is assumed linear. The output $y(t_k)$ is a linear combination of the regressor vector $\mathbf{z}(t_k)$:

$$y(t_k) = \mathbf{d}(p) \mathbf{z}(t_k) \quad (8)$$

By multiplying with $\mathbf{z}^H(t_k)$ and applying the expectation operator, we can write

$$\mathbf{r}_{yz} = \mathbf{d}(p) \mathbf{R}_{zz} \quad (9)$$

We can now estimate the least-squares estimated temperature drift in frame p by using the estimated covariance and cross-correlation matrices

$$\begin{aligned} \hat{\mathbf{R}}_{zz} &= \frac{1}{M} \sum_{k=1}^M \mathbf{z}(k) \mathbf{z}^H(k) \\ \hat{\mathbf{r}}_{yz} &= \frac{1}{M} \sum_{k=1}^M \hat{y}(k) \mathbf{z}^H(k) \end{aligned} \quad (10)$$

and calculate the diagonal elements of $\hat{\mathbf{D}}(p)$ as

$$\hat{\mathbf{d}}(p) = \hat{\mathbf{r}}_{yz} \hat{\mathbf{R}}_{zz}^{-1} \quad (11)$$

Note that the samples used in (10) are not necessarily from the same frame p . The performance will be improved if samples from several frames are used, as discussed below.

The elements in $\hat{\mathbf{d}}(p)$ are low-pass filtered in order to introduce a memory in the algorithm. A first order filter with a pole at 0.9 is used. This will reduce the variance of the regressor vector and therefore improve the tracking of \mathbf{d} . Experiences from the simulations show that this improves the tracking ability. When using this indirect approach instead of the direct method described in Section 3.1, samples from the whole frame is used in the identification process, instead of the utilization of only one sample as in the LMS-approach. Furthermore, mobile communication systems are interference limited and not noise limited. Thus the noise level in $\mathbf{x}(t)$ (and also in $\mathbf{z}(k)$) will be low compared to the signal levels. Therefore $\hat{\mathbf{R}}_{zz}$ will be badly conditioned if the number of incoherent rays impinging on the array is less than N . The calculation of the inverse $\hat{\mathbf{R}}_{zz}^{-1}$ will create problems

when computing $\hat{\mathbf{d}}(p)$ in (11) and the tracking of the temperature drift may not succeed. This can however be mitigated by using a few number of samples from several frames to estimate the covariance matrices. This will in general make $\hat{\mathbf{R}}_{zz}$ better conditioned. The idea is that the fading will cause the signal components in $\mathbf{z}(k)$ to vary over the frames, creating a sequence that is persistently exciting with a well conditioned covariance matrix $\hat{\mathbf{R}}_{zz}$. This approach will thus benefit from a rapidly time-varying signal environment and as opposed to the LMS-approach presented in Section 3.1, which requires a stationary or slowly time-varying signal environment. The reason for this is that here we only track \mathbf{D} which varies more slowly than the weight vector \mathbf{w} .

4 Simulation study

The aim of the simulation is to study the performance of the two auto-calibration algorithms presented above. A simple signal environment with two mobiles transmitting binary phase shift keying (BPSK) modulated signals of equal power but with different training sequences was used. The two signals were transmitting on the same frequency and the wavelength was λ . The desired and the interfering signals are assumed to impinge on an eight element uniform linear array (ULA) from distinct directions θ_d and θ_i respectively. No multipath propagation or fading is assumed. The antenna array inter-element spacing was $\lambda/2$. The length of the training sequence was 26 symbols to comply with the GSM/DCS-1800 standard.

The received signal can be expressed as

$$\mathbf{x}_a(t) = \mathbf{a}(\theta_d) s_d(t) + \mathbf{a}(\theta_i) s_i(t) \quad (12)$$

where $\mathbf{a}(\theta_d)$ and $\mathbf{a}(\theta_i)$ are the array response vectors in direction θ_d and θ_i and $s_d(t), s_i(t)$ are the desired and interfering signals respectively.

In the simulations the temperature drift in magnitude and phase was generated as independent integrated random-walk processes to obtain a ‘‘smooth’’ drift. The elements of the diagonal matrix \mathbf{D} can be written as

$$d_l = A_l e^{j\varphi_l} \quad l = 1, \dots, N \quad (13)$$

Where A_l and φ_l are generated as integrated random walk processes:

$$\begin{aligned} A_l(p+1) &= A_l(p) + \frac{1}{1-q^{-1}} v_{A,l}(p) \\ \varphi_l(p+1) &= \varphi_l(p) + \frac{1}{1-q^{-1}} v_{\varphi,l}(p) \end{aligned} \quad (14)$$

with $v_{A,l}(p)$ and $v_{\varphi,l}(p)$ being white noise sequences of appropriate variance. A_l and φ_l are initialized by the values from the off-calibration. This gives a temperature drift with statistical properties similar to the measurements presented in Figure 1.

To reduce the conditional number (or eigenvalue spread) of the covariance matrix $\hat{\mathbf{R}}_{\mathbf{xx}}$ in (2), regularization is employed to obtain a condition number approximately equal to 10^2 . More details of this regularization method can be found in [8]. The covariance matrix can therefore be inverted without numerical problems, and the weight vector calculated by the SMI-algorithm will be approximately the same from frame to frame, under steady state conditions.

This will support the one frame delay in the weight settings. Since the LMS-algorithm proposed in Section 3.1 is a closed loop algorithm, it is not possible to update the weights more frequently than once per frame; the “response” of the old weights is used to calculate the new weights. This means that the time step of the algorithm is one TDMA frame (or 4.615 ms in GSM/DCS-1800).

The noise variances of the integrated random walk processes (14), that model the temperature drift of the magnitude and the phase, sets the time scale of the simulation and can be increased to reduce the simulation time. It is therefore not necessary to simulate more than 500 frames corresponding to 2.3 seconds in GSM/DCS-1800.

To measure the performance of the adaptive antenna, the SIR on the beamformer output was estimated as

$$\widehat{SIR} = \frac{E(|\hat{\mathbf{w}}^H \mathbf{a}(\theta_d) s_d(t)|^2)}{E(|\hat{\mathbf{w}}^H \mathbf{a}(\theta_i) s_i(t)|^2)} = \frac{|\hat{\mathbf{w}}^H \mathbf{a}(\theta_d)|^2}{|\hat{\mathbf{w}}^H \mathbf{a}(\theta_i)|^2} \quad (15)$$

Here we have assumed that the noise levels are well below the signal levels.

The SIR of the adaptive array utilizing the auto-calibration algorithm presented in Section 3.1 is plotted as a function of frame number in Figure 5. In this particular simulation the angles of the two mobiles have been chosen to $\theta_d = 15^\circ$ and $\theta_i = 43^\circ$ relative to the broadside direction of the ULA. The step size μ used in the LMS-like algorithm was 0.005. The variances of the noise sources σ_1^2, σ_2^2 and σ_3^2 were chosen 20 dB, 40 dB and 30 dB below the signal level, respectively. The SIR of the adaptive array only utilizing the off-line calibration is also plotted in Figure 5 for comparison. It is evident that the auto-calibration algorithm is able to maintain the SIR on a high level, whereas the performance of the traditional SMI adaptive array is severely degraded as the drift in the magnitude and phase of the weights is introduced. The variations of the SIR is also lower for the LMS-method. This is due to the recursion involved in the algorithm that smoothes the SIR.

Figure 6 shows the SIR when using the identification approach presented in Section 3.2, compared to the SMI algorithm with the off-line calibration data only. All simulation parameters are identical to those in the LMS-study. Also in this case the SIR of the auto-calibration algorithm is maintained on a high level. However, the variations of the SIR is higher in this case compared to the LMS-approach, and more

similar to the SMI without drift compensation. This can be explained by the batch oriented approach in the tracking as opposed to the LMS method where the feedback signal smoothes the weight adjustments and the variation of CIR is slower. In the identification approach it is also possible to study the tracking ability of the algorithm. The tracking of the temperature drift for the fifth antenna path is presented in Figure 7, and it can be seen that the tracking of both magnitude and phase is successful.

5 Summary

Two algorithms are proposed for mitigating the temperature drift in adaptive antenna arrays using hardware weights. The two methods utilize a feedback signal from the summed beamformer output. The first method used the initially calculated SMI-weights to create a reference signal in the DSP. An LMS-like algorithm then adjusts the hardware weights to make the feedback signal follow the reference. The second method attempts to track the drift in the transfer functions, and use this tracking information to adjust the SMI-weights. Simulations shows that the output SIR is unaffected for both methods when a realistic temperature drift generated as an integrated random walk process is introduced. The SMI-algorithm without compensation for the temperature drift however suffers a considerable performance degradation. The variance of output SIR of the LMS-approach is lower due to the smoothing effect introduced by the recursive algorithm. The LMS-approach requires a slowly time-varying signal environment. Otherwise the algorithm will lose track of the weight-vector \mathbf{w} . The tracking approach does not demand a slowly varying or quasi-static signal environment as the LMS-approach. It actually benefits from rapid time variations as in a multipath environment. Such variations in the signal environment will tend to make the input signal to the algorithm persistently exciting. As long as the problem of a persistently exciting input signal can be handled, it will therefore be the more attractive approach. It is however more computationally complex.

6 Acknowledgements

We wish to acknowledge Olle Gladh, Leonard Rexberg, Eric Sandberg at Ericsson Radio Access AB for financial and technical support. Bengt-Victor Andersson and Magnus Appelgren at Communicator is acknowledged for consultations regarding the measurements. We would also like to acknowledge Henrik Andersson and Mikael Landing for the development of the adaptive antenna demonstrator. Further we would like to thank the reviewers, who gave useful comments on how to improve the paper. The project has been

References

- [1] L.C. Godara, "Applications of antenna arrays to mobile communications, Part I and II," *Proceedings of the IEEE*, vol. 85, no. 7,8, pp. 1031–1060,1195–1245, 1997.
- [2] P. Zetterberg, *Mobile Cellular Communications with Base Station Antenna Arrays: Spectrum Efficiency, Algorithms and Propagation Models*, PhD thesis, Royal Institute of Technology, Stockholm,Sweden, 1997.
- [3] M.Beach G.Tsoulus, J.McGeehan, "Space division multiple access (SDMA) field trials. Part 2: Calibration and linearity issues," *IEE Proceedings on Radar, Sonar and Navigation*, vol. 145, no. 1, pp. 79–84, 1998.
- [4] M.Beach S.M.Simmonds, "Downlink calibration requirements for the TSUNAMI(II) adaptive antenna testbed," in *Proceedings of the Ninth International Symposium on Personal, Indoor and Mobile Radio Communications*, Boston,USA, 8-11 September 1998.
- [5] J.Strandell, M. Wennström, A.Rydberg, and T.Öberg, "Experimental evaluation of an adaptive antenna for a TDMA mobile telephone system," in *Proceedings of the Eight International Symposium on Personal, Indoor and Mobile Radio Communications*, Helsinki, Finland, 1-4 September 1997, pp. 79–84.
- [6] J.Strandell et.al., "Design and evaluation of a fully adaptive antenna for telecommunication system," in *Antenn 97*, Gothenburg,Sweden, 1997, pp. 357–366.
- [7] JR. R.T. Compton, *Adaptive Antennas*. New Jersey: Prentice-Hall, Inc, 1988.
- [8] B.D. Carlson, "Covariance estimation and diagonal loading in adaptive arrays," *IEEE Transactions on Aerospace and Electronic Systems*, vol. 24, no. 4, pp. 397–401, 1988.

List of Figures

1	Temperature drift of hardware weight	8
2	Block diagram of the adaptive antenna	9
3	Block diagram of the LMS-approach. <i>FSRX</i> =Feedback Sampling Receiver, <i>ISRX</i> =Input Sampling Receiver. <i>T</i> represents one frame delay	10
4	Identification model	11
5	SIR as a function of frame number. Dash-dotted: auto-calibration using LMS, solid: SMI with off-line calibration data only	12
6	SIR as a function of frame number. Dashed: auto-calibration using the identification approach, solid: SMI with off-line calibration data only	13
7	Tracking of variations in magnitude and phase for the fifth antenna path obtained from the identification method. Dashed: tracked drift, solid: true drift	14

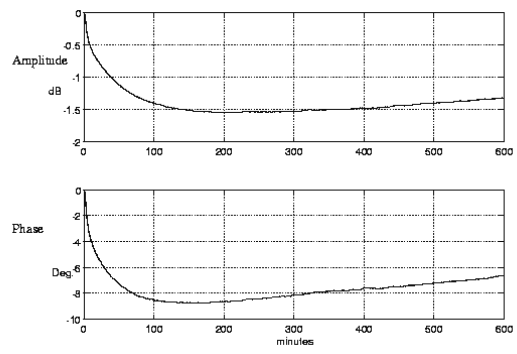


Figure 1: Temperature drift of hardware weight

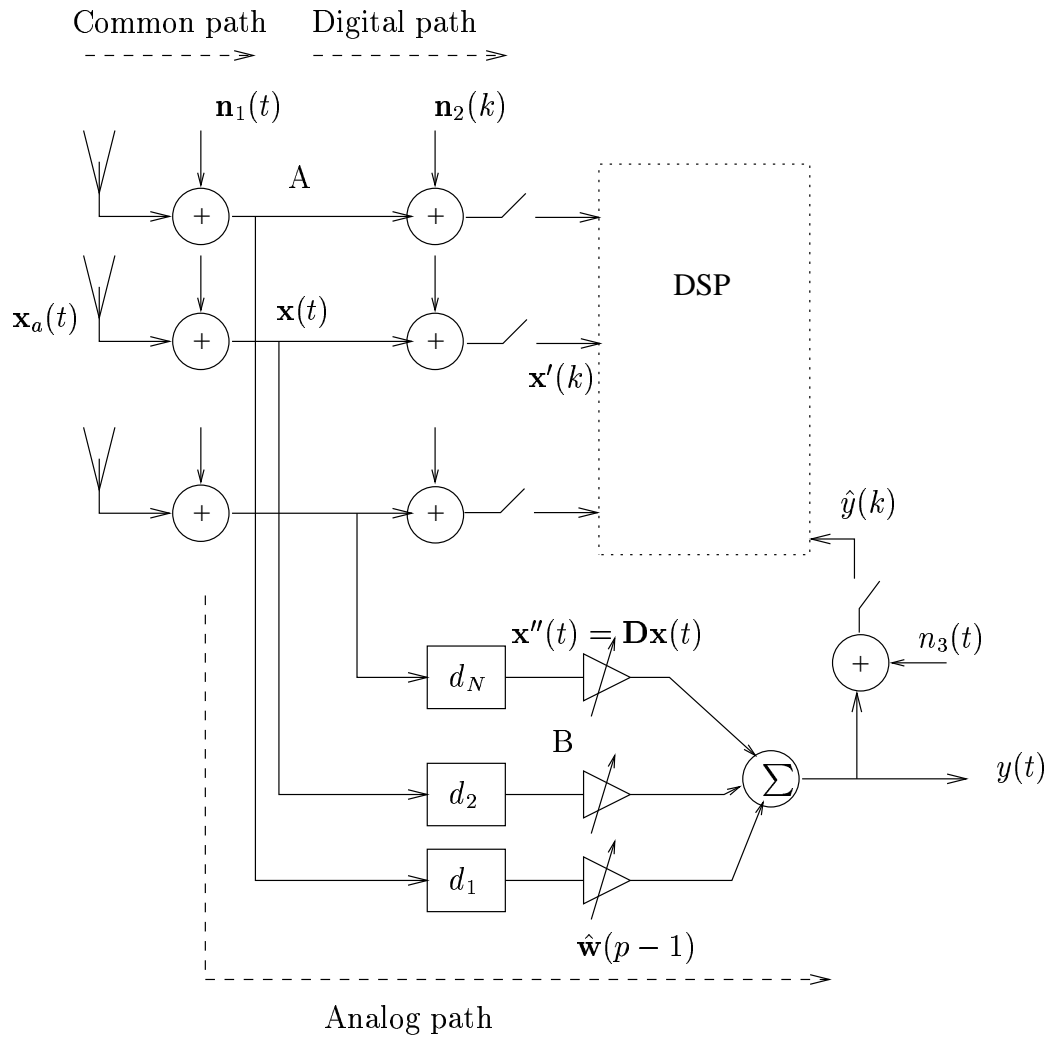


Figure 2: Block diagram of the adaptive antenna

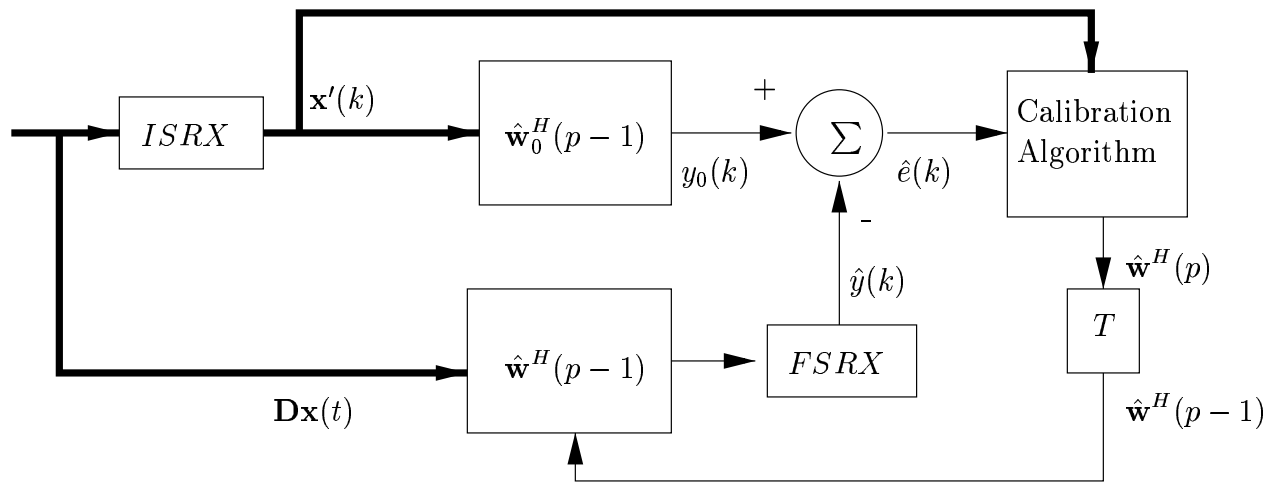


Figure 3: Block diagram of the LMS-approach. *FSRX*=Feedback Sampling Receiver, *ISRX*=Input Sampling Receiver. *T* represents one frame delay

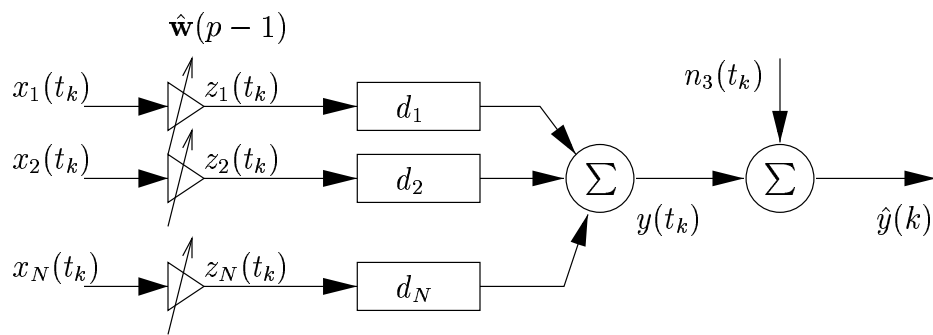


Figure 4: Identification model

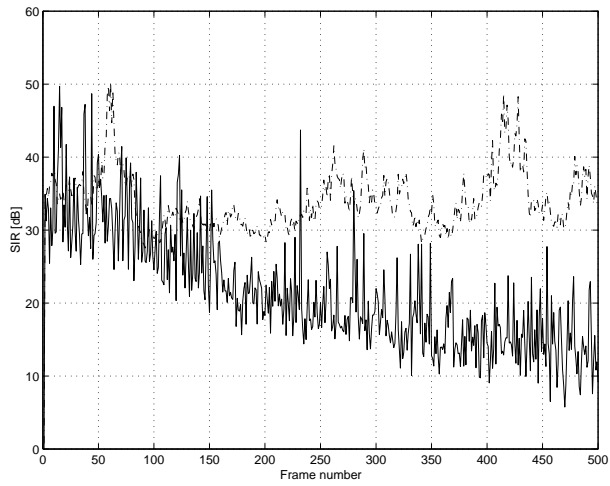


Figure 5: SIR as a function of frame number. Dash-dotted: auto-calibration using LMS, solid: SMI with off-line calibration data only

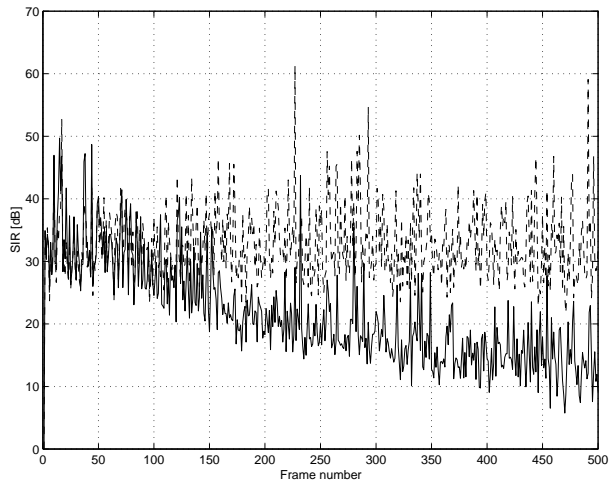


Figure 6: SIR as a function of frame number. Dashed: auto-calibration using the identification approach, solid: SMI with off-line calibration data only

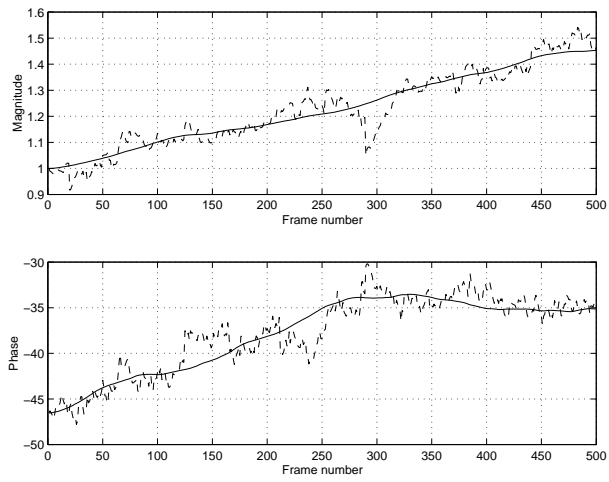


Figure 7: Tracking of variations in magnitude and phase for the fifth antenna path obtained from the identification method. Dashed: tracked drift, solid: true drift